CHEMISTRY OF MATERIALS

VOLUME 15, NUMBER 8 APRIL 22, 2003

Articles

Computer Simulation Study of the Effect of Surface Pre-Relaxation on the Adhesion of Apatite Thin Films to the (0001) Surface of α-Quartz

Nora H. de Leeuw*,†,‡ and Donald Mkhonto§

School of Crystallography, Birkbeck College, University of London, Malet Street, London WC1E 7HX, U.K., Department of Chemistry, University College, University of London, 20 Gordon Street, London WC1H 0AJ, U.K., and Materials Modeling Center, University of the North, Sovenga, South Africa

Received November 12, 2002. Revised Manuscript Received January 27, 2003

Computer simulations of apatite thin films at a range of α-quartz surfaces have shown how the strength of adhesion between thin films of apatite material and ceramic silica surfaces is crucially dependent upon both the orientation of the film relative to the substrate and the nature of the silica surface − a finding which is important in a wide number of applications, from basic geological research into intergrowth of phosphate and silicate rock minerals to the search for more effective surgical implant materials. It is shown that although the unrelaxed quartz surface is more reactive toward the apatite film, the more regular thin film structures grown at the pre-relaxed quartz surfaces lead to more stable interfaces. Interfacial energies for a single apatite layer range from 0.64−1.22 Jm^{-2} at the unrelaxed quartz surface to 0.55−0.73 Jm^{-2} at the relaxed surface. Hence, the nature of the substrate surface before attachment of the film is more important in determining the structure and stability of the resulting interface than the initial reactivity of the substrate and/or the degree of bonding between the two materials across the interface. In addition, film growth at the unrelaxed quartz surface is energetically increasingly unfavorable, whereas growth at the pre-relaxed surface is calculated to continue beyond the first layer and we predict that the apatite thin film will form local domains of both (2 × 2) as well as clockwise and anticlockwise (2 × 2)R120° adsorbate layers.

Introduction

A major area in the contemporary field of materials science is the study of adhesion of thin films to inorganic surfaces. A topical example is in the field of biomaterials science where deposition and layer growth of synthetic bone materials, such as apatite, onto a ceramic implant may promote integration of the implant with the natural bone;[1] but to date it is unclear how the apatite attaches to the implant material. Apatites Ca_{10}-

* To whom correspondence should be addressed. E-mail: n.deleeuw@mail.cryst.bbk.ac.uk.
† School of Crystallography, Birkbeck College, University of London.
‡ Department of Chemistry, University College, University of London.
§ Materials Modeling Center, University of the North.

(1) Cho, S. B.; Miyaji, F.; Kokubo, T.; Nakanishi, K.; Soga, N.; Nakamura, T. *J. Mater. Sci − Mater. Med.* **1998**, *9*, 279.

10.1021/cm021359k CCC: $25.00
Published on Web 03/22/2003

$(PO_4)_6(F,Cl,OH)_2$ are a complex and diverse class of materials, where the isomorphous series can be represented by fluorapatite $Ca_{10}(PO_4)_6F_2$, which is by far the most common, chlorapatite $Ca_{10}(PO_4)_6Cl_2$, hydroxyapatite $Ca_{10}(PO_4)_6(OH)_2$, and carbonate-apatite $Ca_{10}(PO_4,CO_3,OH)_6(F,OH)_2$.[2] They are the most abundant phosphorus-bearing materials and are found in almost all igneous rocks and to a lesser extent in sedimentary and metamorphic rocks. In geological situations, apatites are often used as geo- and thermo-chronometers, either by measuring fission tracks of thorium and uranium,[3−5] argon dating,[6] or the retention of ^{4}He, the decay product of uranium and thorium.[7,8] In addition, the presence and isotopic composition of noble gases, such as helium, xenon, and argon, in apatites can give insight into mantle processes in the past.[9,10] Furthermore, because of their affinity for impurity ions, apatites may well become important as environmental sinks for the uptake of heavy metals and radioactive contaminants, such as lead and uranium.

More recently, apatites have gained additional prominence due to their biological role as one of the main constituents of mammalian bones and teeth enamel, and they are becoming increasingly important as candidates for use as bio-materials.[11] As such, they may be valuable in the manufacture of artificial bones, while another possible application is the use of ceramic implants as a support for the crystallization and layer growth of apatite, aiding the acceptance of the implant material by the body. For this latter application, synthetic apatite is found to nucleate and grow on the surfaces of ceramic silicate implants which then bond to the living bone through these apatite layers.[12,13] However, as the precise nature of the apatite thin film is not known there is a clear need to gain an understanding of the interactions between the apatite layers and the ceramic substrate at the atomic level. In addition, understanding of the interface between complex materials is of increasing significance in itself. The present work reports detailed atomistic models for the interfaces between apatite and α-quartz based on computer simulation methods.

Methodology

Computational methods are well placed to calculate at the atomic level the geometries and adhesion energies of solid/solid interfaces. In this theoretical study of the interfacial structure between apatite and silicate implants, we have concentrated on α-quartz as a model for a range of silicate materials and silica-rich bioglasses. Our approach is to employ classical energy minimization techniques to study the interactions of thin films of fluorapatite, the major apatite phase, with the α-quartz basal plane, which was calculated to be the most stable quartz surface.[14] These atomistic simulation methods are based on the Born model of solids,[15] which assumes that the ions in the crystal interact via long-range electrostatic forces and short-range forces, including both the repulsions and the van der Waals attractions between neighboring electron charge clouds. The long-range Coulombic interactions are calculated using the Parry technique[16,17] (which is adapted from the well-known Ewald method for 2D periodic systems) whereas the short-range forces are described by parametrized analytical expressions. The electronic polarizability of the ions is included via the shell model of Dick and Overhauser[18] in which each polarizable ion, in our case the oxygen and fluorine ions, is represented by a core and a massless shell, connected by a spring. The polarizability of the model ion is then determined by the spring constant and the charges of the core and shell, which are usually obtained by fitting to experimental dielectric constants when available. In addition, it is often necessary to include angle-dependent forces to allow for directionality in partially covalent bonds, for instance in the silica groups and phosphate anion. We employed an established potential model for the silicate substrate[19] and newly developed potentials for apatite, which have been shown to be accurate in describing both bulk and surface properties of the material.[20] The potential parameters describing the interactions between the apatite film and silicate surface (Table 1) were derived following the approach of Schroder et al.[21] which has been shown to be a reliable method for potential derivation and adjustment where no experimental data are available, e.g., as in references 22 and 23.

We used the METADISE computer simulation code for calculation of the surface and adsorbate structures and energies,[24] as it is designed to model dislocations, interfaces, and surfaces. Following the approach of Tasker,[25] the crystal is described as a series of charged planes parallel to the surface/interface and periodic in two dimensions; it is then divided into two blocks each comprising two regions, region I and region II. Region I contains those atoms near the extended defect, in this case the surface or solid−solid interface and a few layers immediately below; these atoms are allowed to relax to

(2) Deer, W. A.; Howie, R. A.; Zussman, J. *An Introduction to the Rock-Forming Minerals*; Longman: Harlow, Essex, UK, 1992.
(3) Romer, R. L. *Geochim. Cosmochim. Acta* **1996**, *60*, 1951.
(4) Menzies, M.; Gallagher, K.; Yelland, A.; Hurford, A. J. *Geochim. Cosmochim. Acta* **1997**, *61*, 2511.
(5) Corfu, F.; Stone, D. *Geochim. Cosmochim. Acta* **1998**, *62*, 2979.
(6) Pellas, P.; Fieni, C.; Trieloff, M.; Jessberger, E. K. *Geochim. Cosmochim. Acta* **1997**, *61*, 3477.
(7) Wolf, R. A.; Farley, K. A.; Silver, L. T. *Geochim. Cosmochim. Acta* **1996**, *60*, 4231.
(8) Farley, K. A.; Wolf, R. A.; Silver, L. T. *Geochim. Cosmochim. Acta* **1996**, *60*, 4223.
(9) Sasada, T.; Hiyagon, H.; Bell, K.; Ebihara, M. *Geochim. Cosmochim. Acta* **1997**, *61*, 4219.
(10) Warnock, A. C.; Zeitler, P. K.; Wolf, R. A.; Bergman, S. C. *Geochim. Cosmochim. Acta* **1997**, *61*, 5371.
(11) Narasaraju, T. S. B.; Phebe, D. E. *J. Mater. Sci.* **1996**, *31*, 1.
(12) Kokubo, T. *Acta Mater.* **1998**, *46*, 2519.
(13) Miyaji, F.; Iwai, M.; Kokubo, T.; Nakamura, T. *J. Mater. Sci − Mater. Med.* **1998**, *9*, 61.
(14) de Leeuw, N. H.; Higgins, F. M.; Parker, S. C. *J. Phys. Chem. B* **1999**, *103*, 1270.
(15) Born, M.; Huang, K. *Dynamical Theory of Crystal Lattices*; Oxford University Press: Oxford, U.K., 1954.
(16) Parry, D. E. *Surf. Sci.* **1975**, *49*, 433.
(17) Parry, D. E. *Surf. Sci.* **1976**, *54*, 195.
(18) Dick, B. G.; Overhauser, A. W. *Phys. Rev.* **1958**, *112*, 90.
(19) Sanders, M. J.; Leslie, M.; Catlow, C. R. A. *J. Chem. Soc. Chem. Commun.* **1984**, 1271.
(20) Mkhonto, D.; de Leeuw, N. H. *J. Mater. Chem.* **2002**, *12*, 2633.
(21) Schröder, K. P.; Sauer, J.; Leslie, M.; Catlow, C. R. A. *Chem. Phys. Lett.* **1992**, *188*, 320.
(22) de Leeuw, N. H.; Parker, S. C. *J. Chem. Soc., Faraday Trans.* **1997**, *93*, 467.
(23) de Leeuw, N. H.; Parker, S. C.; Hanumantha Rao, K. *Langmuir* **1998**, *14*, 5900.
(24) Watson, G. W.; Kelsey, E. T.; de Leeuw, N. H.; Harris D. J.; Parker, S. C. *J. Chem. Soc., Faraday Trans.* **1996**, *92*, 433.
(25) Tasker, P. W. *Philos. Mag. A* **1979**, *39*, 119.

Table 1. Potential Parameters Used in This Work (Short-Range Cutoff 20 Å)

Charges (e)

ion	core	shell	core−shell interaction (eVÅ^{-2})
Ca	+2.000		
P	+1.180		
F	+1.380	−2.380	101.2000
phosphate oxygen (Op)	+0.587	−1.632	507.4000
silicate oxygen (Os)	+0.84819	−2.84819	74.92038

Buckingham Potential

ion pair	A (eV)	ρ (Å)	C (eVÅ^6)
Ca−Op	1550.0	0.29700	0.0
Ca−Os	2966.5	0.29700	0.0
Ca−F	1272.8	0.29970	0.0
Si−F	2545.6	0.29970	0.0
Si−Os	1283.91	0.32052	10.66158
Si−Op	670.9	0.32052	3.76
Op−Op	16372.0	0.21300	3.47
Os−Os	22764.3	0.14900	27.88
Op−Os	16372.0	0.21300	3.47
Op−F	583833.7	0.21163	7.68
Os−F	1117385.1	0.21163	14.6
F−F	99731834.0	0.12013	17.02423

Morse Potential

	D (eV)	α (Å^{-1})	r_0 (Å)
$P_{core}-Op_{core}$	3.47	1.900	1.600

Three-Body Potential

	k (eV rad^{-2})	Q_0
$Op_{core}-P-Op_{core}$	1.322626	109.47
$Os_{shell}-Si-Os_{shell}$	2.09724	109.47

their mechanical equilibrium. Region II contains those atoms further away, which represent the rest of the crystal and are kept fixed at their bulk equilibrium position. The energies of the blocks are essentially the sums of the energies of interaction between all atoms. It is necessary to include region II to ensure that the total interaction energy of an ion at the bottom of region I is modeled correctly. The bulk of the crystal is simulated by the two blocks together while a surface is represented by a single block with the top of region I as the free surface. A solid/solid interface is created by fitting two surface blocks together in different orientations. Both regions I and II need to be sufficiently large for the energy to converge apart from the thin film, which only consists of region I, where all ions are allowed to relax explicitly.

The energy minimization techniques employed in this work are the most suitable techniques to investigate at the atomic level these solid/solid interfaces between two complex materials, which necessitates large simulation cells containing thousands of ions. These techniques are now well-established in the field of solid state chemistry, especially in ionic solids where the van der Waals interactions play an important role, and they have been shown to be successful in the accurate structure and energy determination and prediction of a wide range of solids,[26] defects,[27] surfaces,[28] solid/solid[29] and solid/liquid interfaces,[30] and surface adsorption.[31]

Table 2. Adhesion Energies (γ_{adh} in Jm^{-2}) for the Interfaces between Single and Double Films of Apatite at the Unrelaxed and Pre-Relaxed α-Quartz Substrate, Calculated with Respect to the Relaxed Quartz Surface and Bulk Apatite (Equation 1)

rotation of film	unrelaxed α-quartz surface		relaxed α-quartz surface	
	thin layer	thick layer	thin layer	thick layer
0°/360°	0.74	1.31	0.58	0.83
60°	0.90	1.50	0.57	1.05
120°	1.07	1.62	0.57	0.89
180°	0.64	1.53	0.73	0.83
240°	1.22	1.62	0.55	0.82
300°	0.72	1.72	0.65	1.11

Results and Discussion

Both α-quartz and apatite have hexagonal crystal structures, where the basal (0001) planes were calculated to be the dominant surfaces.[2,32] We therefore decided to use the α-quartz (0001) surface as the substrate for the layer growth of apatite material, also in the (0001) orientation although the apatite thin films have to accommodate themselves to the α-quartz surface lattice vectors. α-Quartz has lattice parameters of $a = b = 4.913$ Å, $c = 5.404$ Å, whereas the lattice parameters of fluorapatite are $a = b = 9.360$ Å, $c = 6.880$ Å.[33] We therefore had to grow the quartz substrate to a 2×2 surface supercell, $a = b = 9.826$ Å, which could accommodate an overlayer of apatite with a misfit of −4.7%. We calculated the adhesion energies for the interface as a function of rotation of the apatite layer with respect to the underlying quartz substrate. The adhesion energy γ_{adh} is a measure of the stability of the interface with respect to the free quartz (0001) surface and bulk apatite, which is calculated as follows:

$$\gamma_{adh} = \frac{E_{int} - (E_{surf,quartz} + E_{bulk,apatite})}{A} \qquad (1)$$

where E_{int} is the energy of the interfacial system, $E_{surf,quartz}$ is the energy of the free quartz surface, $E_{bulk,apatite}$ is the energy of the relevant number of bulk apatite units in the film, and A is the area of the interfacial region. The calculated adhesion energies are shown in Table 2, where the most stable interface has the lowest value of γ_{adh}. We calculated the adhesion energy with respect to the apatite units in the bulk material as we are interested in the formation and stability of a thin apatite film on the substrate surface, rather than the intergrowth of two materials. For example, if we were to investigate the intergrowth of two rock minerals in geological applications, the calculation of the interfacial stability with respect to the free surfaces of both quartz and apatite would be more appropriate. However, this calculation would only add a constant term to each of the different columns of

(26) Lewis, D. W.; Bell, R. G.; Wright, P. A.; Catlow, C. R. A.; Thomas, J. M. *Stud. Surf. Sci. Catal.* **1997**, *105*, 2291
(27) Wright, K.; Catlow, C. R. A. *Phys. Chem. Miner.* **1994**, *20*, 515.
(28) Oliver, P. M.; Parker, S. C.; Egdell, R. G.; Jones, F. H. *J. Chem. Soc., Faraday Trans.* **1996**, *92*, 2049.
(29) Harding, J. H.; Harris, D. J.; Parker, S. C. *Phys. Rev. B* **1999**, *60*, 2740.
(30) de Leeuw, N. H.; Watson, G. W.; Parker, S. C. *J. Phys. Chem.* **1995**, *99*, 17219.
(31) de Leeuw, N. H.; Parker, S. C.; Rao, K. H. *Langmuir*, **1998**, *14*, 5900.
(32) Elliott, J. C. *Structure and Chemistry of the Apatites and Other Calcium Orthophosphates*, Studies in Inorganic Chemistry 18; Elsevier: Amsterdam, The Netherlands, 1994.
(33) Hendricks, S. B.; Jefferson, M. E.; Mosley, V. M. *Z. Kristall. Kristallgeom. Kristallphys. Kristallchem.* **1932**, *81*, 352.

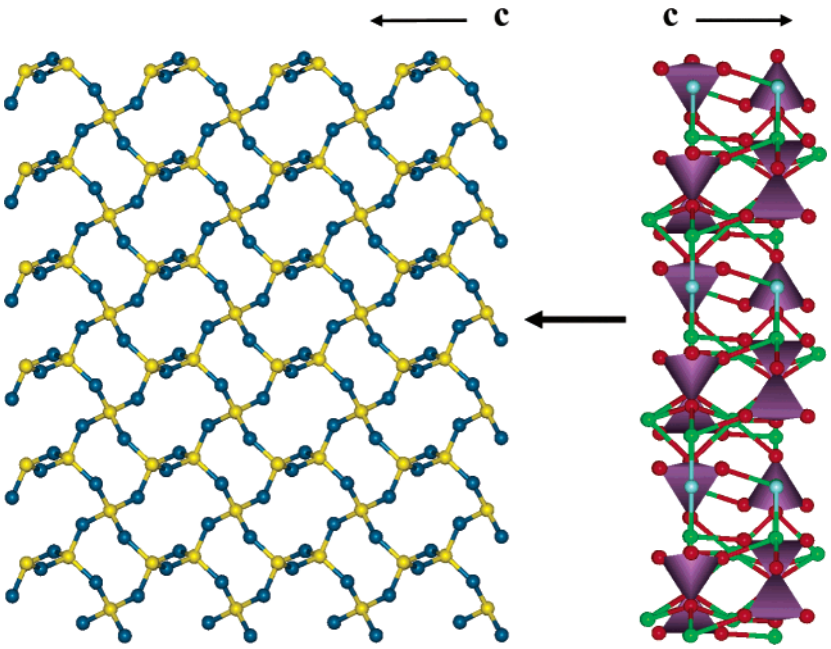

Figure 1. Diagram showing how a thin layer of fluorapatite is brought down upon the unrelaxed quartz (0001) surface (Si = yellow, O_{quartz} = dark blue, $O_{apatite}$ = red, F = pale blue, P = purple, Ca = green, PO_4 groups shown as tetrahedra).

adhesion energies in Table 2, rather than alter the relative energies and hence stabilities of the interfaces, which would remain the same. We therefore do not quote both values.

Lateral Scanning of Apatite film over Quartz Surface. Figure 1 shows the unrelaxed α-quartz and apatite crystal structures, showing the F^- ions in the apatite structure located one above the other in a column parallel to the *c*-axis. These fluoride ions are surrounded by calcium ions in hexagonal channels, whereby each F^- is coordinated to three calcium ions in the same a−b plane. Figure 1 further indicates how the apatite thin film was brought down upon the quartz (0001) surface. Before energy minimization of the interfacial system, the apatite film was kept at a constant height above the surface, but moved laterally with respect to the quartz surface without relaxation of the substrate or film; i.e. for the interface shown in Figure 1, the apatite film would be moved systematically in the a- and b-directions and the interfacial energy for this unrelaxed system would be calculated for a series of points on a grid. The grid was determined by the surface lattice vectors of the system in the a- and b-directions, in this case 9 Å in the a-direction and 8 Å in the b-direction, and the interfacial energy was calculated at intervals of 1 Å. This scan thus supplied us with an interfacial energy at each point on the grid, hence identifying the lowest energy relative lateral displacement of the film with respect to the substrate in the unrelaxed system. This configuration was then taken as our starting point for the energy minimization calculation of the substrate/film interface, which for the 0° rotated interface shown in Figure 1 was at $a = 3$ Å and $b = 3$ Å. In addition, the grid of energies supplied us with an energy contour map of the unrelaxed interfacial energy with respect to lateral position of the film above the substrate, an example of which is shown in Figure 2 for the 0° rotated interface of Figure 1, which also identifies lowest energy pathways for moving the film over the substrate. Once the most energetically favorable initial lateral film/substrate orientation was thus identified, a full geometry optimization was performed to obtain the energy of the relaxed interfacial system. The optimization algorithm used was the Newton−Raphson variable matrix method, which takes into account not only the first derivative of the energy with respect to ion position, i.e., the forces on the ions during minimization, but also the second derivative of the energy. The initial height above the surface was varied in a series of calculations to check that this parameter did not affect the final energy and to ensure that the lowest energy configuration had been obtained. During geometry optimization, not only was the apatite film free to move in any direction with respect to the underlying quartz surface, but all atoms in the apatite film and in a quartz surface region of about 22 Å into the bulk (region I) were also completely unconstrained so as not to prejudice the geometry of the interface. The complete process was then repeated for a series of rotations of the apatite thin film with respect to the quartz substrate and the adhesion energies calculated (Table 2).

Previous computational studies of solid−solid interfaces, whether grain boundaries in geological systems (e.g., refs 34 and 35) or thin films of catalytic materials (e.g., ref 36) have always started their calculations from unrelaxed interfaces, i.e. where the two blocks of material were initially fitted together as bulk-terminated blocks before, only then, allowing the interface to relax in an energy minimization or molecular dynamics simulation. However, in experiment, the substrate relaxes instantaneously upon formation of the surface,[37] well before attachment of the film; we therefore inves-

(34) de Leeuw, N. H.; Parker, S. C.; Catlow, C. R. A.; Price, G. D. *Am. Mineral.* **2000**, *85*, 1143.
(35) Harding, J. H.; Harris, D. J.; Parker, S. C. *Phys. Rev. B* **1999**, *60*, 2740.
(36) Sayle, D. C.; Catlow, C. R. A.; Harding, J. H.; Healy, M. J. F.; Maicaneanu, S. A.; Parker, S. C.; Slater, B.; Watson, G. W. *J. Mater. Chem.* **2000**, *10*, 1315.
(37) Attard G.; Barnes, C. *Surfaces*; Oxford University Press: Oxford, U.K., 1998.

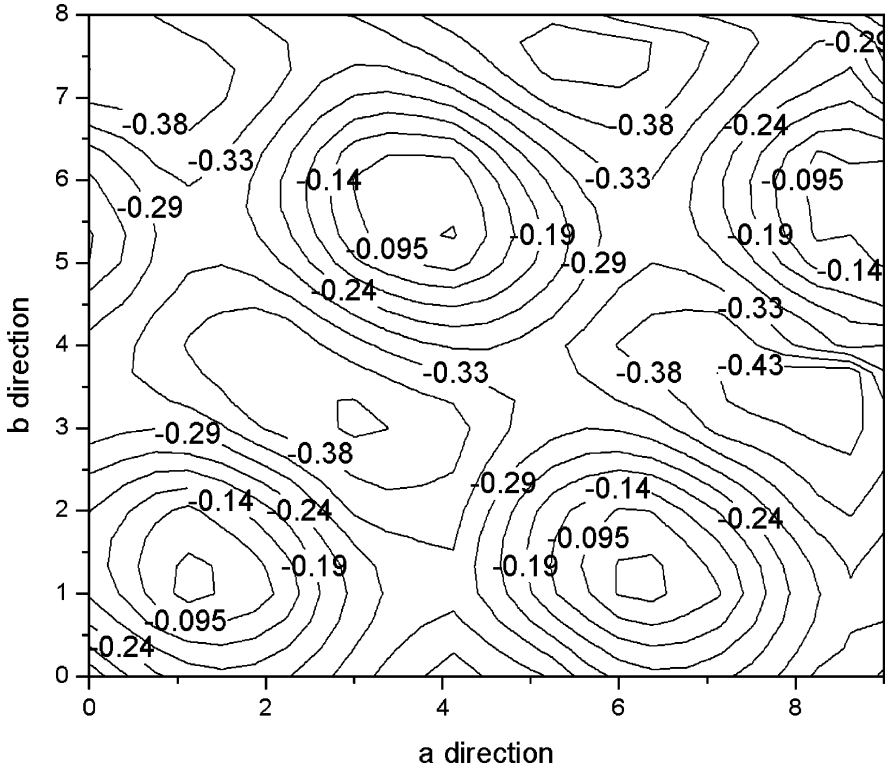

Figure 2. Contour map of the interfacial energies of the unrelaxed quartz/apatite system with respect to lateral position, from a horizontal scan of the unrelaxed 0° rotated apatite film over the unrelaxed quartz {0001} surface (energies shown in eV, the units on the axes are distances in Å along the surface a- and b-vectors of the simulation cell).

tigated whether pre-relaxation of the substrate before attachment of the film significantly affected the interfacial structures and energies or whether the final structures and energies would be the same, regardless of the starting configuration of the substrate surface. In the former case we would need to include surface pre-relaxation in these and future interfacial calculations to ensure that the correct structures and energies are calculated. We hence considered both the interfaces between substrate and film starting from a bulk-terminated α-quartz surface and from a pre-relaxed α-quartz surface.

Adhesion at the Unrelaxed Quartz Surface. We first fitted a single apatite layer to the quartz substrate, where the quartz surface was kept as a bulk-terminated plane which had not been relaxed before creating the interface. Comparing the structures of the interfaces due to the different rotations, we observed that the stability of the interface as given by its adhesion energy depends on a number of factors. The number of bonds that can form between the calcium and oxygen ions of the apatite film and oxygen and silicon ions respectively in the quartz substrate plays a role, but more so the lengths of the bonds. For example, the 0° rotational interface forms only two bonds per apatite unit cell to the underlying quartz structure, one O−Si bond of 1.80 Å and one Ca−O bond of 2.36 Å, whereas the 60° rotation forms several Ca−O and O−Si bonds, which are all, however, longer than 2.50 and 1.84 Å, respectively, and as we see from Table 2 the 60° interface is much less stable. The most stable interface at a rotation of 180°, shown in Figure 3, contains both a large number of bonds between the film and substrate, which are also short (O−Si 1.68−1.83 Å, Ca−O 2.41−2.56 Å), and often the oxygen or calcium ions form multiple bonding across the interface. The other factor that determines the stability of the interface is the size of the empty region between substrate and film. In the 180° rotation, the film fits closely to the substrate and the interfacial region is relatively dense. For example, the gap between the topmost quartz silicon atom and the bottom calcium atom in the apatite layer is only 2.25 Å wide (in the c-direction only, the closest actual Ca−Si distance is 3.85 Å). As we can see from Figure 3, the oxygen atoms of both quartz substrate and apatite layer are located in the interfacial area, forming a network of close interactions between both materials. In the less stable interfaces, on the other hand, larger interfacial cavities and channels are formed, which destabilizes these interfacial regions. The same effect is seen to occur in rock grain boundaries, where large cavities lead to unstable grain boundary regions, which become stable only when the cavities collapse or are filled with interstitial species such as water molecules.[34]

Adhesion of Double Thickness Films at the Unrelaxed Quartz Surface. Following our simulations of single apatite layers on the quartz substrate, we also studied the interfacial structures and energies of a series of thicker apatite films of two unit cells deep (∼14 Å). From the adhesion energies in Table 2, it is clear that the effect of the increased thickness is to destabilize the interfaces in all cases. In addition the relative stabilities of the rotations, have changed as we see that the 0° rotation rather than the 180° is now the preferred configuration for the apatite film. The spread in adhesion energies is also less than that for the single apatite layer, varying by ±15% from the average of 1.55 Jm^{-2}. The higher adhesion energies and their relative invariance across the series of rotations is due to a lesser flexibility of the double apatite layer. The ions in the

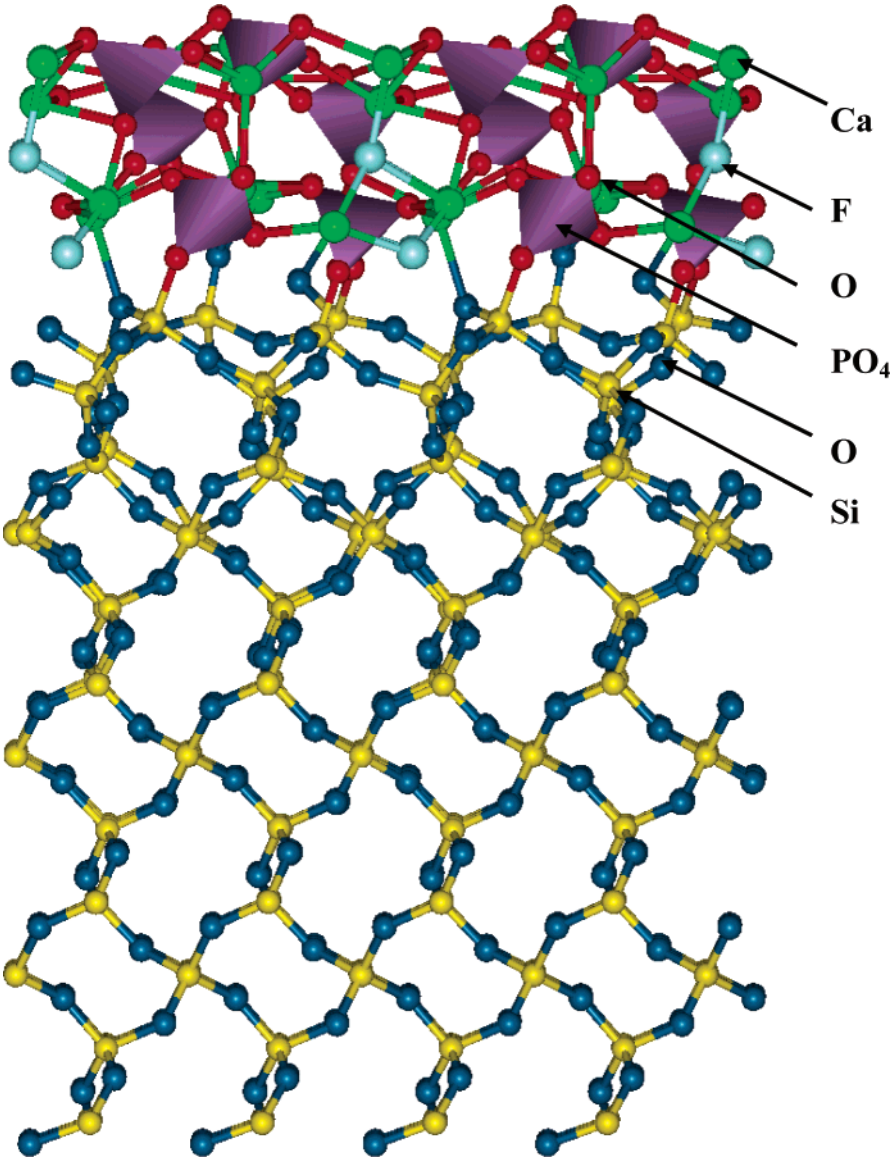

Figure 3. Geometry-optimized structure of a single layer of apatite film grown onto the unrelaxed quartz (0001) surface at a rotation of 180°, showing rotation of the PO_4 groups and distortion of the F chains (Si = yellow, O_{quartz} = dark blue, $O_{apatite}$ = red, F = pale blue, P = purple, Ca = green, PO_4 groups shown as tetrahedra).

thicker film are more constrained to remain in an environment which is approximating the apatite crystal structure, although stretched to accommodate itself to the underlying quartz lattice. For example, whereas in the single layers the PO_4 groups had rotated freely and the columns of fluoride ions had become severely distorted in the a- and b-directions (e.g., Figure 3), in the thicker film the basic structure of the apatite lattice remains intact and is similar to the unrelaxed structure shown in Figure 1. The PO_4 groups are no longer rotated with respect to the apatite lattice and the fluoride ions remain in regular columns, one above the other in the c-direction.

Adhesion at the Pre-Relaxed Quartz Surface. We finally considered growing single and double apatite layers on a pre-relaxed quartz surface and compared these calculations with the previous simulations of the bulk-terminated substrate surfaces. The main difference between the unrelaxed and relaxed quartz surfaces is the presence of dangling bonds on the unrelaxed surface, where the surface silicon and oxygen atoms have a lower coordination than in the bulk material. The surface silicon atoms are only coordinated to three oxygen atoms, while the oxygen atoms are forming just a single bond to one surface silicon atom each (shown in Figure 4(a)). Upon relaxation the surface Si and O atoms form bonds parallel to the surface and hence regain their bulk coordination numbers of four and two respectively, which is shown in Figure 4(b). As a result of this surface relaxation and recovery of the bulk coordination of the surface ions, the unrelaxed and pre-relaxed surfaces are not identical and we may therefore expect that they will interact with the apatite films in different ways, which is indeed observed. As a result of the dangling bonds, the unrelaxed quartz surface is highly reactive toward the apatite film, forming bonds from the undercoordinated surface species to oxygen and calcium atoms in the apatite film, as discussed above and shown in Figure 3. However, we saw that this enhanced reactivity of the substrate leads to irregular and distorted structures of the apatite films and, to a lesser extent, the quartz surface. Conversely, when the quartz surface is relaxed

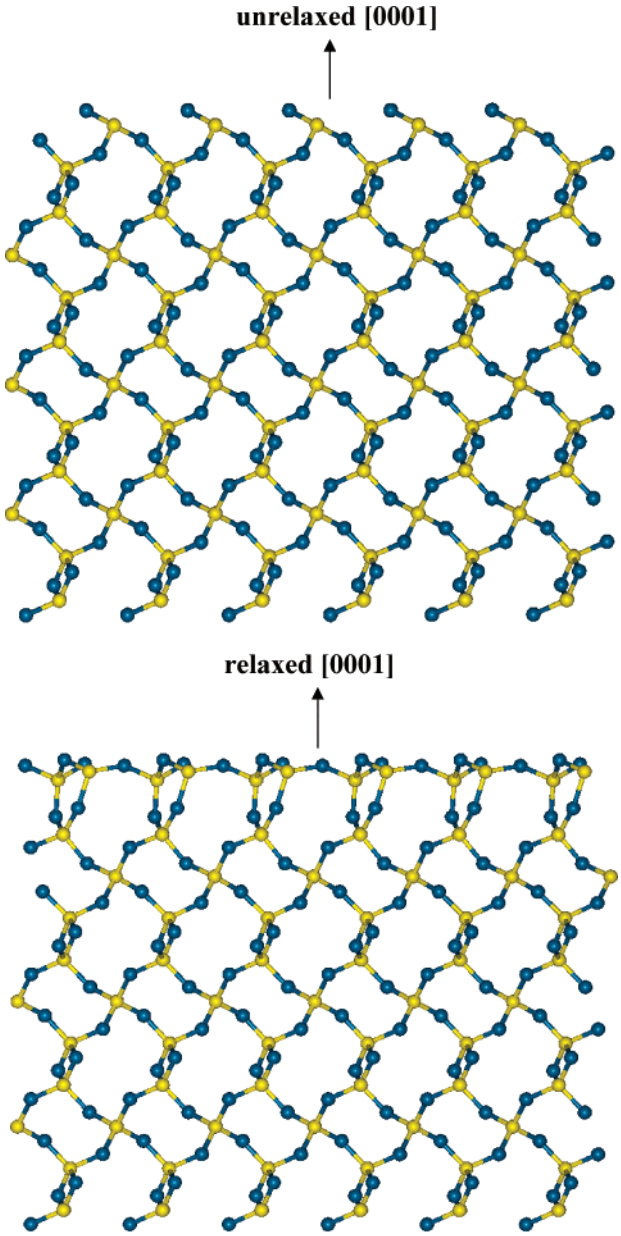

Figure 4. Unrelaxed (a) and relaxed (b) α-quartz (0001) surface, showing low-coordinated surface Si and O species on the unrelaxed surface, which upon relaxation have regained their 4-fold and 2-fold bulk coordination number for Si and O respectively (Si = yellow, O = blue).

before attachment of the apatite thin film, the structure of the quartz surface does not alter significantly upon adhesion of the apatite film. The silicon and oxygen atoms retain their 4- and 2-fold coordination to the O and Si atoms in the quartz surface, rather than form bonds to calcium and oxygen atoms in the apatite thin film. The interactions which are formed between the quartz surface and the apatite thin film are therefore much weaker as they are over and beyond the normal coordination number of the oxygen and silicon atoms in the substrate, with much longer $Si-O_{apatite}$ (≥ 2.02 Å) and $Ca-O_{quartz}$ (≥ 2.52 Å) distances than we found when the substrate was not pre-relaxed. The interfacial gap between the two materials is also much wider. The closest distance between oxygen atoms of the two materials is 1.79 Å in the c-direction (actual closest $O_{quartz}-O_{apatite}$ distance is 2.78 Å) whereas for the

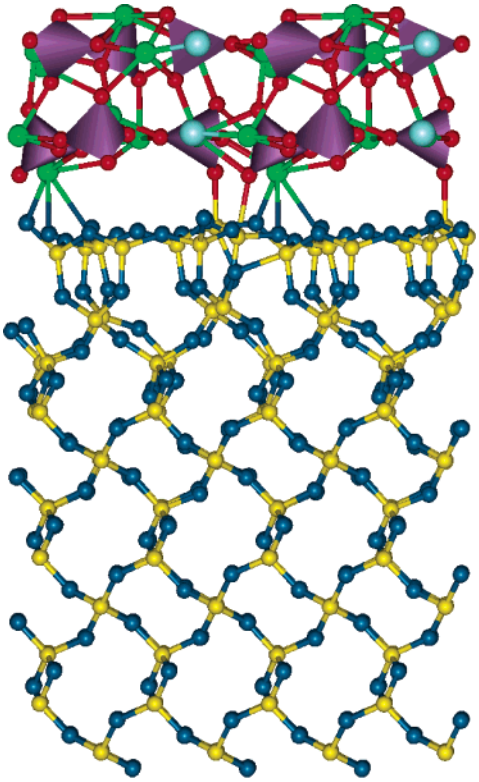

Figure 5. Geometry-optimized structure of a single layer of apatite film grown onto the relaxed quartz (0001) surface at a rotation of 240°, showing $Ca-O_{quartz}$ distances up to 2.5 Å and $O_{apatite}-Si$ distances up to 3.0 Å (Si = yellow, O_{quartz} = dark blue, $O_{apatite}$ = red, F = pale blue, P = purple, Ca = green, PO_4 groups shown as tetrahedra).

unrelaxed substrate we saw that oxygen atoms from the two materials mixed in the interfacial region.

However, we see from Table 2 that despite the lower reactivity of the relaxed quartz surface and the more open structure of the interfacial region, the energies of adhesion of the two film thicknesses to the pre-relaxed quartz surface are generally lower than those for the unrelaxed quartz surface and hence these interfaces are more stable. It is also noteworthy that the adhesion energies fall in a fairly narrow band, especially for the thin layer where they are within 9% of the average adhesion energy. The enhanced stabilities of these interfaces and the similarities in the interfacial energies are due to the fact that the apatite layer attached to the pre-relaxed quartz surface (shown in Figure 5 for the 240° rotation) is much less distorted than at the unrelaxed quartz surface. Consequently, when the thickness of the apatite film is increased from a single to a double layer, this does not enforce a significant change in the structure of the apatite film, as was seen at the unrelaxed quartz surface, and as a result the same rotation of 240° (shown in Figure 6) remains the preferred configuration. This behavior, unlike the adhesion of apatite layers on the unrelaxed quartz surface where the rotation of 180° was preferred for the thin film, but a rotation of 0° was preferred once the apatite was more constrained in the thicker film, shows that the apatite film once formed at the pre-relaxed surface could easily be grown in a layer by layer deposition, which agrees with experimental findings where apatite is found to grow at silicate surfaces.[12,13]

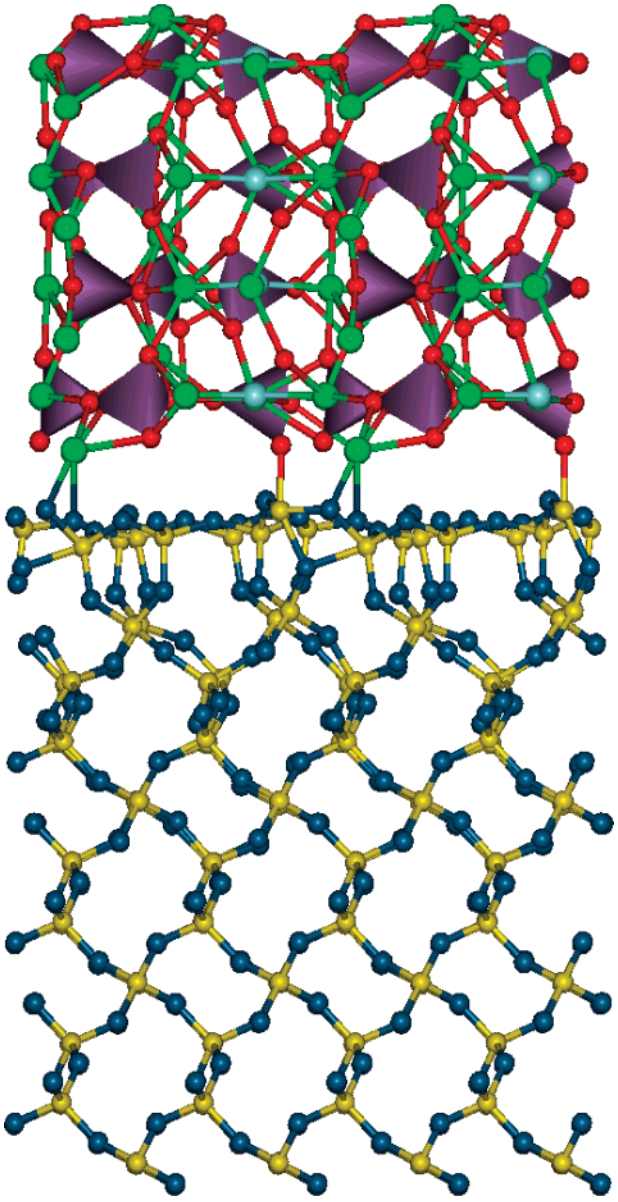

Figure 6. Geometry-optimized structure of a double-layer apatite film grown onto the relaxed quartz (0001) surface at a rotation of 240° (Si = yellow, O_{quartz} = dark blue, $O_{apatite}$ = red, F = pale blue, P = purple, Ca = green, PO_4 groups shown as tetrahedra).

Conclusions

In this computer modeling study of a range of interfaces between two complex oxide materials, we have shown how the stability and orientation of the apatite thin film is determined by the nature of the bonding between the materials across the interface. Although the unrelaxed quartz surface is more reactive toward the apatite film, this effect is outweighed by the regularity of the thin film structures grown at the pre-relaxed surfaces, and as a result the interfacial energies are more favorable when the quartz surface is pre-relaxed. Figure 7 shows a graph of the adhesion energies for the four films as a function of rotation of the apatite film with respect to the substrate surface, from which

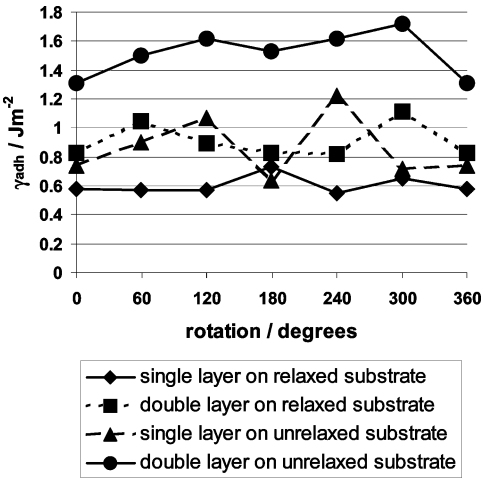

Figure 7. Adhesion energies as a function of rotation of the apatite film with respect to the quartz surface.

it is clear that the films grown at the unrelaxed surface vary widely in stability, and they are generally far less stable than those grown at the relaxed surface. In addition, film growth beyond the first apatite layer is energetically increasingly unfavorable at the unrelaxed substrate surface. Conversely, at the pre-relaxed surface, the increase in interfacial energies with increase in film thickness begins to converge, especially at the lowest energy rotations, and we could therefore expect film growth to continue. It is clear from our simulations that the nature of the substrate surface before attachment of the film is more important in determining the final structure and stability of the resulting interface than the initial reactivity of the substrate and/or the degree of bonding between the two materials across the interfacial.

On the basis of our calculated adhesion energies, we predict that the apatite thin film will form local domains of both (2 × 2) as well as clockwise and anticlockwise (2 × 2)R120° adsorbate layers. Apatite films formed at unrelaxed quartz surfaces lead to significantly more distorted and less stable interfaces, in addition to giving different lowest energy rotations. Hence, if we are to interpret experimental findings correctly and predict growth behavior and energies for use in film deposition onto inorganic surfaces, the nature of the substrate surface needs to be included in the computer simulations.

Future work will include investigating the interface of apatite thin films grown on hydroxylated α-quartz surfaces and molecular dynamics simulations of the interfaces to study the effect of temperature.

Acknowledgment. N.H.dL. thanks the EPSRC for an Advanced Research Fellowship and acknowledges the Wellcome Trust (grant 065067) and NERC (grant NER/M/S/2001/00068) for funding. D.M. thanks Prof. P. Ngoepe for useful discussions and acknowledges the Royal Society and the NRF and CSIR South Africa for financial support.

CM021359K